



Molecular docking and NMR binding studies to identify novel inhibitors of human phosphomevalonate kinase

Pornthip Boonsri^{a,b}, Terrence S. Neumann^{a,1}, Andrew L. Olson^{a,2}, Sheng Cai^a, Timothy J. Herdendorf^c, Henry M. Miziorko^c, Supa Hannongbua^{b,*}, Daniel S. Sem^{a,*}

^aChemical Proteomics Facility at Marquette, Department of Chemistry, Marquette University, Milwaukee, WI 53201, United States

^bDepartment of Chemistry, NANOTEC Center of Nanotechnology, National Nanotechnology Center, Faculty of Science, Kasetsart University, Bangkok 10900, Thailand

^cDivision of Molecular Biology and Biochemistry, School of Biological Sciences, University of Missouri-Kansas City, Kansas City, MO 64110, United States

ARTICLE INFO

Article history:

Received 17 October 2012

Available online 10 November 2012

Keywords:

Human phosphomevalonate kinase

Inhibitors

Virtual screening

Molecular docking

ABSTRACT

Phosphomevalonate kinase (PMK) phosphorylates mevalonate-5-phosphate (M5P) in the mevalonate pathway, which is the sole source of isoprenoids and steroids in humans. We have identified new PMK inhibitors with virtual screening, using autodock. Promising hits were verified and their affinity measured using NMR-based ¹H–¹⁵N heteronuclear single quantum coherence (HSQC) chemical shift perturbation and fluorescence titrations. Chemical shift changes were monitored, plotted, and fitted to obtain dissociation constants (*K_d*). Tight binding compounds with *K_d*'s ranging from 6–60 μM were identified. These compounds tended to have significant polarity and negative charge, similar to the natural substrates (M5P and ATP). HSQC cross peak changes suggest that binding induces a global conformational change, such as domain closure. Compounds identified in this study serve as chemical genetic probes of human PMK, to explore pharmacology of the mevalonate pathway, as well as starting points for further drug development.

© 2012 Elsevier Inc. All rights reserved.

1. Introduction

Phosphomevalonate kinase (PMK), a mevalonate pathway enzyme, catalyzes a key phosphorylation step in isoprenoid/sterol biosynthesis, and provides a variety of products that are necessary for normal cellular growth and signaling, such as cholesterol, bile acids, heme A, dolichol, and ubiquinone [1]. Due to the central role of isoprenoids, imbalances in isoprenoid synthesis and utilization can lead to cellular dysfunction and disease [2–4]. Inhibitors of two enzymes in this pathway are of particular clinical relevance. The statins, a large class of hydroxymethylglutaryl-CoA reductase (HMG CoA) inhibitors, are widely used to treat elevated cholesterol levels [5]. And, bisphosphonate inhibitors of farnesyl pyrophosphate synthase are used to treat metabolic bone disease [6].

Abbreviations: PMK, phosphomevalonate kinase; M5P, mevalonate-5-phosphate; HSQC, Heteronuclear single quantum coherence; HMG CoA, hydroxymethyl glutaryl-CoA reductase.

* Corresponding authors. Present address: School of Pharmacy, Center for Structure-based Drug Design and Development, Concordia University, Mequon, WI 53097, United States. Fax: +1 262 243 2752 (D.S. Sem).

E-mail address: daniel.sem@cuw.edu (D.S. Sem).

¹ Present address: School of Pharmacy, Center for Structure-based Drug Design and Development, Concordia University, Mequon, WI 53097, United States.

² Present address: Department of Molecular & Structural Biochemistry, North Carolina State University, Raleigh, NC 27695, United States.

However, the mechanism and pharmacology of other potentially druggable enzyme targets in this pathway are less well-characterized, so additional studies and pharmacological probes are needed [7].

PMK is comprised of two domains. The larger ATP-binding domain (CORE, Fig. 1) is composed of a five stranded parallel β-sheet interweaved with three α-helices. The mevalonate-5-phosphate (M5P) domain (substrate, Fig. 1) is composed of loop regions and two α-helices. PMK catalyzes the transfer of a phosphoryl group from adenosine-5'-triphosphate (ATP) to M5P, resulting in mevalonate-5-pyrophosphate and adenosine diphosphate (ADP) [8–12]. While details of the protein motion that occurs during catalysis remain unclear, the LID (Fig. 1) region is likely involved in an opening and closing motion to permit the binding and release of substrates [13–15]. Herdendorf and Miziorko investigated the functional role of conserved basic residues in human PMK and suggested that R110 was important for human PMK catalysis [16]. R111 and R84 are situated close to the “Walker B” motif and seem to be involved in binding M5P [16]. Residues K100 and K101 are in close proximity to the ATP binding site, and likely stabilize the transition state for conversion of ATP to ADP [17,18].

In this study, we aim to identify novel inhibitors with high affinity for human PMK, based on our understanding of important protein–ligand interactions that involve the above-mentioned basic residues. These inhibitors could provide clues as to the relative

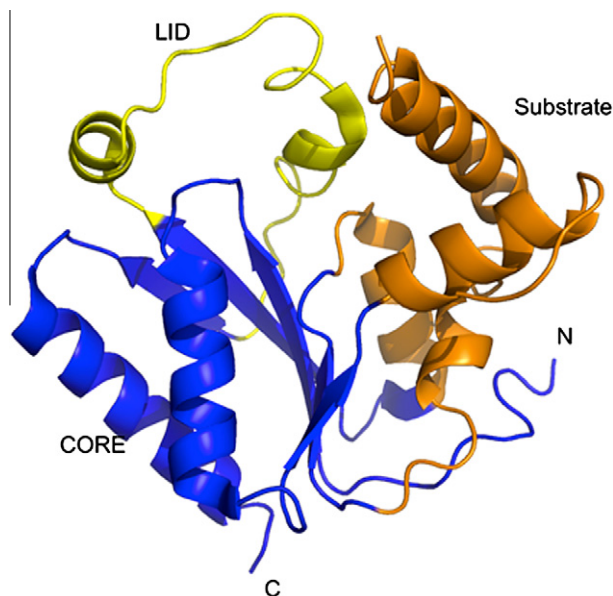


Fig. 1. Crystal structure of human PMK (PDB ID 3ch4) [22] showing the different functionally relevant regions of the protein. The LID region caps the active site where phosphate transfer occurs, and contains catalytic residues needed for stabilizing the negative charge buildup in the phosphate transfer transition state. The CORE and Substrate domains are proposed to participate in significant domain rearrangements upon binding the substrates MSP and MgATP [15].

importance of binding interactions, and could themselves be useful as chemical probes of function (ex. in cellular assays or *in vivo*). Molecular docking has become an important early-stage method for finding novel inhibitors, when a protein structure is available [19,20]. The process allows a large number of chemicals to be tested quickly *in silico*, and promising chemicals can then be prioritized for experimental verification of binding *in vitro* [21]. Given the high false-positive rate of docking predictions, it is crucial to verify predicted binding affinity using experimental assays. Two PMK structures have been published, allowing for docking-based identification of inhibitors [2,22].

NMR methods allow for a comprehensive monitoring of the effects of ligand binding, by providing chemical shift change measurements that reflect structural changes throughout the entire protein. Of particular interest, the ^1H – ^{15}N HSQC experiment can provide an effective method for monitoring changes to a protein structure upon substrate or inhibitor addition, based on changes to ^1H – ^{15}N chemical shifts of all the protein backbone amides [23]. Since PMK is known to undergo substrate-induced structural changes [24], solution NMR techniques are well-suited to study interactions involving the human PMK/ligand complexes, which may also involve ligand-induced global structural rearrangements, such as the domain closure that substrate binding induces. Using molecular docking, solution NMR techniques, and fluorescence titrations, we identified novel inhibitors of human PMK. By monitoring ^1H – ^{15}N HSQC chemical shift perturbations, site specific molecular interactions were identified and characterized.

2. Materials and methods

2.1. Virtual screening protocol

Chemicals to be docked were sourced from two datasets: an in-house collection of 10,000 drug-like compounds, previously purchased or synthesized for kinase and oxidoreductase studies, and ChEMBL, a Thai Natural Products collection containing 1000 structures [25,26]. Before docking, ligands were adjusted to the proper protonation state at pH 7.4 by Pipeline Pilot, ver. 7.4 [27],

and three-dimensional structures were calculated using Corina [28]. Molecular docking experiments were performed with AutoDock 4.2 [29–31].

The structure of human PMK (PDB ID: 3CH4) was obtained from the Protein Data Bank [22]. Gasteiger charges and hydrogens were added using AutoDock Tools (ADT). The docking grid, centered on the MSP binding pocket, was also prepared using ADT with a grid box created using $60 \times 60 \times 60$ points and a resolution of 0.375 Å.

2.2. Protein expression and purification

Human PMK is a 192-residue protein with a molecular weight of 22.0 kDa. To aid in purification, a hexa-histidine tag was added at the N-terminus resulting in a total molecular weight of 24.2 kDa. Human PMK cDNA was purchased from OriGene, subcloned into the pET15b expression plasmid, expressed, and purified as described previously [8]. Briefly, the expression plasmid was transformed into *Escherichia coli* BL21 (DE3) Rosetta cells (Novagen) which encoded human PMK. Then, cells were grown in 1 L of Luria–Bertani (LB) media containing ampicillin (amp) and chloramphenicol (chl) until the optical cell densities at 600 nm (OD_{600}) reached 0.7. The cells were harvested by centrifugation for 15 min at 6000g. These cells were suspended in minimal media with amp–chl antibiotics supplemented with ^{15}N – NH_4Cl (Sigma Aldrich) as the lone source of nitrogen [32]. Cells were allowed to acclimate for 1 h, and then they were induced with 1 mM IPTG. Cells were harvested 4 h after induction by centrifugation. Cell pellets were re-suspended in a buffer containing 50 mM potassium phosphate, 5 mM imidazole, 5% glycerol, 1 mM phenylmethanesulfonylfluoride (PMSF), and 300 mM NaCl at pH 7.8. Cells were lysed by passage through in a microfluidizer at ~ 17 kpsi. The lysate was clarified by centrifugation at 15,000 rpm for 30 min, and the supernatant loaded onto 1 mL of a Ni-Sepharose Fast-Flow resin (GE Healthcare). The column was washed with the 50 mM phosphate buffer until $A_{280} < 0.005$, and the protein was eluted using the same buffer supplemented with 300 mM imidazole. Protein concentration was determined spectrophotometrically using an extinction coefficient (ϵ_{280}) of $32,290 \text{ M}^{-1} \text{ cm}^{-1}$ calculated with Expasy ProtParam and the amino acid sequence [33].

2.3. NMR sample preparation and spectroscopy

Protein was concentrated to 400–600 μM by using a 10 kDa cut-off centricon (AMD Millipore) filter and exchanged into a buffer containing 20 mM potassium phosphate, 5 mM dithiothreitol (DTT), 100 mM potassium chloride, 10% glycerol, 0.02% sodium azide, and 10% D_2O , at pH 6.5. All screened compounds were dissolved in d_6 -dimethyl sulfoxide (DMSO) to a concentration of 5 mM. Titrations were performed using 100 μM increments. Spectra were compared to control experiments of PMK and d_6 -DMSO (Supplementary Figure 2). Crosspeaks without a d_6 -DMSO effect on ^1H – ^{15}N HSQC chemical shifts were monitored and used to calculate K_d values. NMR experiments were performed at 25 °C using a Varian 600 MHz NMR system at 599.515 MHz using a triple resonance probe, with actively shielded Z-gradients. NMR data were processed and visualized by using NMRPipe [34] and analyzed with NMRview [35]. Dissociation constants (K_d) were calculated by from chemical shift changes resulting from conversion of free PMK, to the various bound states, as described previously [15]. The peaks that were monitored were in fast exchange in both ^1H and ^{15}N dimensions. Chemical-shift perturbations from NMR titrations were quantified using Eq. (1),

$$\Delta\text{shift}_{\text{obs}} = \left[({}^1\text{Hshift})^2 + \left(\frac{{}^{15}\text{Nshift}}{6.51} \right)^2 \right]^{0.5} \quad (1)$$

Then, the K_d value was determined by plotting and fitting (Graph-Pad Prism ver. 4.00 [36]) the chemical shift changes ($\Delta\text{shift}_{\text{obs}}$) as a function of the concentration of protein and ligand, using the quadratic equation in Eq. (2),

$$\Delta\text{shift}_{\text{obs}} = \left(\frac{\Delta\text{shift}_{\text{max}}}{2[P_0]} \right) \left[([L_0] + [P_0] + K_d) - \left(([L_0] + [P_0] + K_d)^2 - 4[L_0][P_0] \right)^{0.5} \right] \quad (2)$$

where L_0 and P_0 are the total ligand concentration at a particular point and protein concentration, respectively, while $\text{shift}_{\text{max}}$ is the

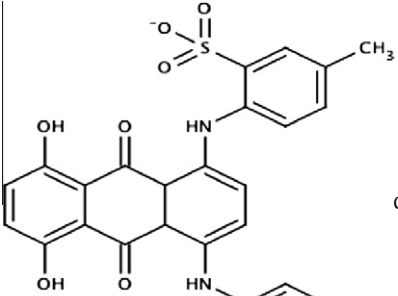
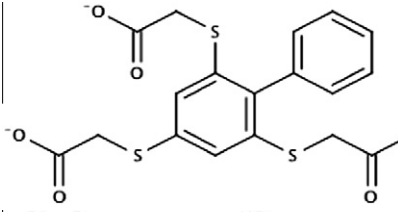
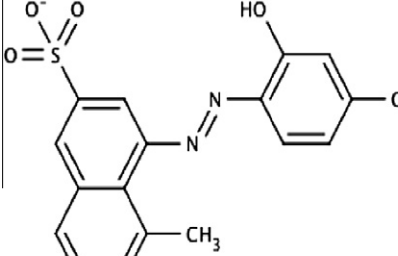
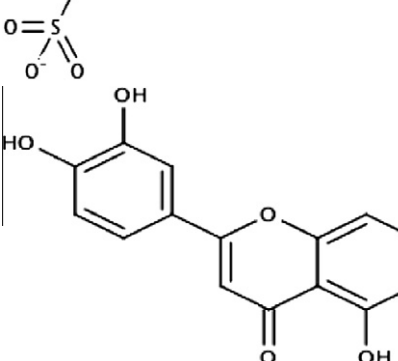
maximum chemical shift change observed for the particular peak of interest.

2.4. Fluorescence titration

Fluorescence titrations were performed at 25 °C, using a Jasco FP-6500 spectrofluorometer. The fluorescence emission of human PMK was measured in a total volume of 0.4 mL of buffer containing 20 mM potassium phosphate, 5 mM DTT, 100 mM potassium chloride, 10% glycerol at pH 6.5 and 5 μM human PMK. Excitation was performed at 295 nm, and emission was recorded at 300–400 nm.

Table 1

Predicted and experimental binding affinity for compounds identified using Autodock 4.2 to dock compounds into human PMK. NMR and fluorescence techniques were then used to experimentally verify binding, and determine dissociation constants (K_d values).

Chemical	Predicted lowest binding energy (kcal/mol)	K_d (μM) NMR [residue used for data fitting]	K_d (μM) fluorescence
 CSDDD_1633	−11.6	55.4 ± 12.9 [G177]	31 ± 8
 CSDDD_2260	−10.34	6.3 ± 5.7 [T128]	14.6 ± 4.6
 CSDDD_2419	−11.8	ND ^a [Q136]	12 ± 2
 luteolin	−9.2	ND ^a [A172]	61.0 ± 19.5

^a The NMR fit was not reliable because in addition to a specific binding event that seems to occur at low concentrations, there is also a non-specific effect that does not plateau.

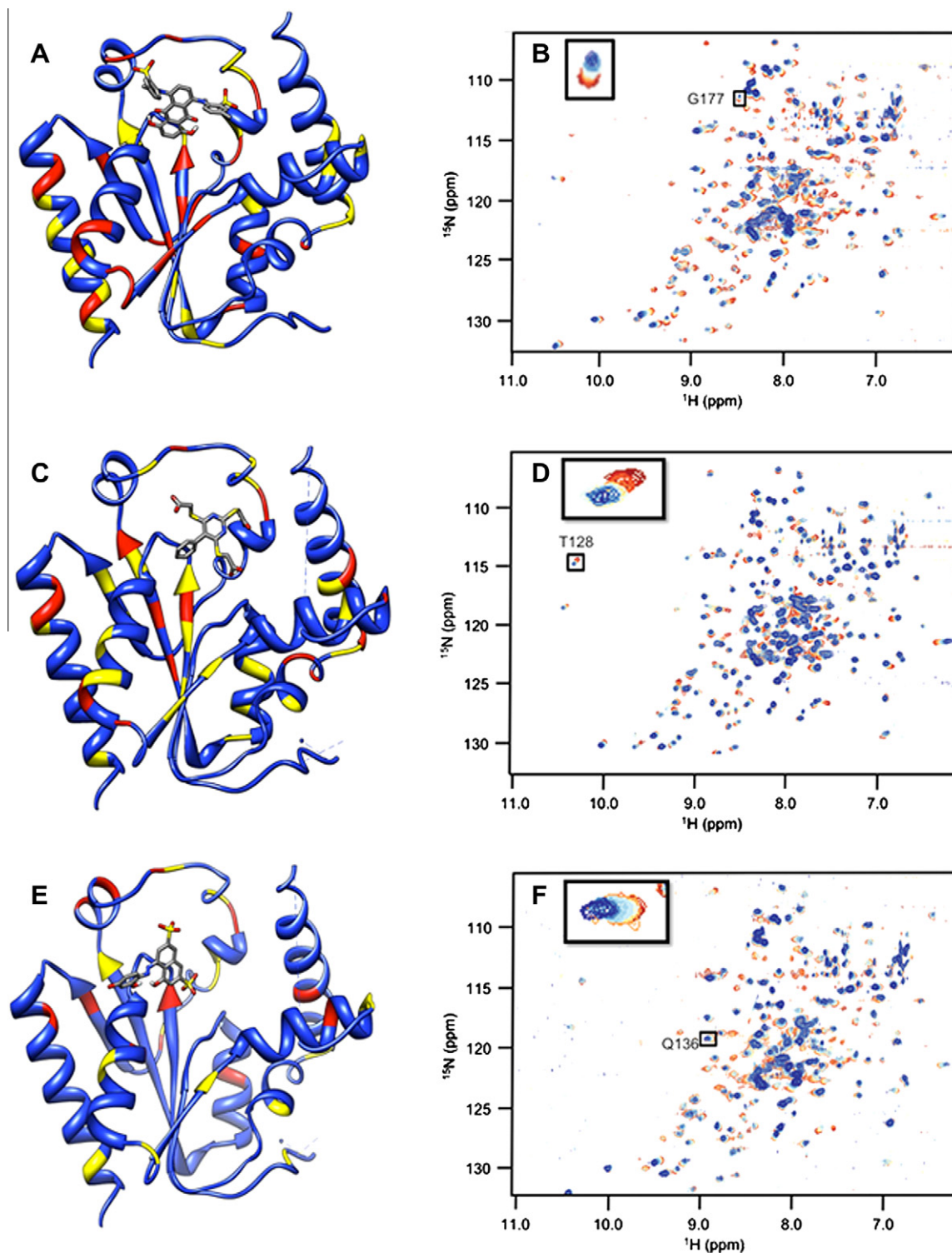


Fig. 2. Chemical shift perturbations due to binding of the inhibitors identified from the synthetic compound collection. ^1H – ^{15}N HSQC spectra chemical shifts are mapped onto the human PMK crystal structure [22], with the predicted binding pose from Autodock for each ligand; chemical shift changes are color-coded such that red is a large (>0.09 ppm) chemical shift change, yellow is a medium (0.05–0.09 ppm) chemical shift change, and blue indicates small or no chemical shift change. Inset panels show chemical shift changes that were used to fit binding data (Eqs. (1) and (2)). Panels A and B are for compound CSDDD_1633, C and D are for compound CSDDD_2260, and E and F are for compound CSDDD_2419.

To determine the K_d , the difference in intensity between bound and free states at each data point were monitored and fitted as a function of ligand concentration to the one-site specific binding equation using GraphPad Prism ver. 4.00 [36].

3. Results

Chemicals from the two sources (synthetic and natural products) were prioritized for experimental screening based upon

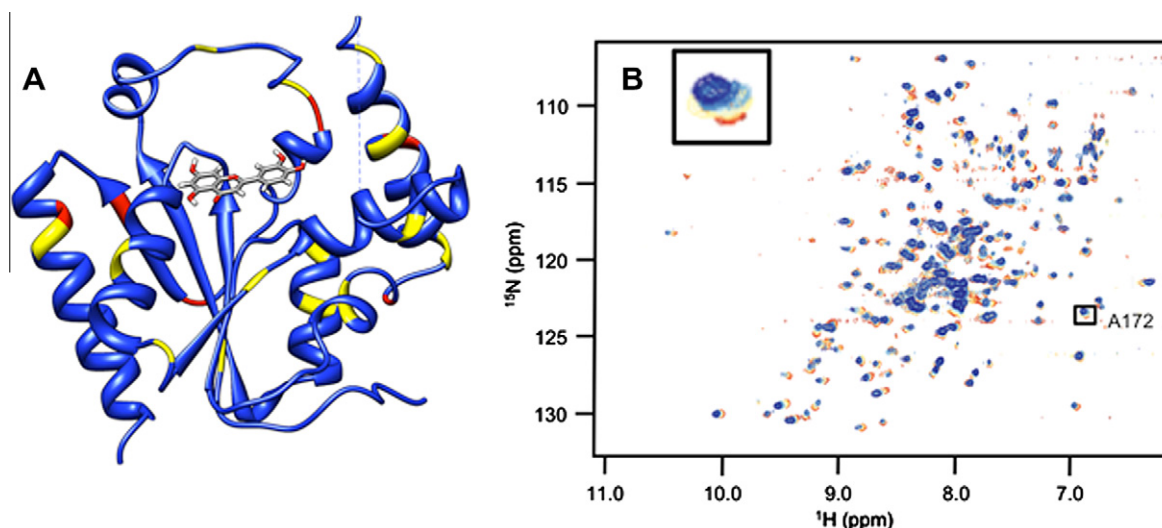


Fig. 3. Chemical shift perturbations due to binding of an inhibitor (luteolin) from the Thai Natural Products compound collection, Chemiebase [25,26]. ^1H – ^{15}N HSQC spectra chemical shifts (Panel B) are mapped onto the human PMK crystal structure (Panel A) [22], with the predicted binding pose from Autodock shown; chemical shift changes are color-coded such that red is a large (>0.09 ppm) chemical shift change, yellow is a medium (0.05 – 0.09 ppm) chemical shift change, and blue indicates small or no chemical shift change. The inset panel shows chemical shift changes that were used to fit binding data (Eqs. (1) and (2)).

docking scores and cluster size, from Autodock 4.2 virtual screening. In total, 26 compounds were identified and then screened using NMR ^1H – ^{15}N HSQC titration experiments; and, chemical shift changes were monitored upon addition of ligand aliquots. Four of these 26 chemicals (15%) showed measurable affinity for PMK in the NMR assay, so fluorescence titrations were also performed for these four compounds to confirm their binding to PMK. Binding affinities for these experiments are summarized in Table 1 and binding fits are provided in Supplementary Figure S1 and S2.

In an attempt to identify the location of inhibitor binding, chemical changes were mapped onto the human PMK crystal structure (PDB ID: 3ch4). In Fig. 2, the 2D ^1H – ^{15}N HSQC spectra and chemical shift mapping are shown for 3 the chemicals sourced from the in house collection of synthetic compounds. Fig. 3 depicts this information for the hit obtained from the Chemiebase collection of Thai natural products.

4. Discussion

The studies presented herein identified four novel inhibitors of PMK, which could lead to pharmacologically useful chemical probes or perhaps even drug leads that target the mevalonate pathway via inhibition of PMK. Molecular docking provided a prioritized listing of chemicals with potential affinity for PMK, with chemicals selected from two chemical collections, an in-house collection of synthetic compounds, and Chemiebase [25,26], a Thai natural product collection. Hits were identified from each chemical source and experimentally validated using NMR ^1H – ^{15}N HSQC and fluorescence experiments. Of compounds predicted to bind to PMK using Autodock, 15% were verified by two methods (NMR and fluorescence) as being actual ligands for PMK. It is noteworthy that NMR titration methods are inherently limited in that they do not provide accurate measures of K_d values, when the K_d value is much less than the protein concentration that must be used in the experiment (which is itself limited by experimental sensitivity of the HSQC experiment). In these situations, data fitting to determine K_d must be done using a quadratic equation (Eq. (2)), and errors increase as $K_d \ll [\text{protein}]$. But, NMR chemical shift perturbation data will confirm binding and provide an upper limit for a K_d even

in these situations, and more accurate K_d values can then be obtained with fluorescence titrations.

Docking and subsequent titrations (NMR and fluorescence) identified three synthetic compounds from the in-house compound collection (CSDDD library) with K_d values in the 12–30 μM range (fluorescence), Table 1. A common feature of these compounds is the presence of negative charges, which could mimic the negative charge on the phosphate groups of the natural substrates, ATP and M5P. Indeed, Autodock 4.2 placed these ligands (Fig. 2(A), (C) and (E)) near the LID and CORE regions of the protein, close to the highly basic region of the known binding site for the natural substrates. Likely, these inhibitors are taking advantage of the strong electrostatic interactions with positively charged amino acids in the vicinity, including K17, R18, K19, K22, R138, and R141. Each of the three in-house collection inhibitors bind tightly to human PMK (Table 1) and these affinities favorably compare to those of the natural substrates ATP ($29 \pm 6 \mu\text{M}$) and ADP ($19.9 \pm 9.0 \mu\text{M}$) [15]. When plotting the chemical shift perturbations for two chemicals (Supplementary Fig. S3), complex binding was observed that could not be accounted for by the quadratic binding model used herein. In the case of CSDDD_2419, (Supplementary Fig. S4) the binding fit showed a nonspecific effect in addition to an initial binding event that appears to be saturable. These additional effects can be detected using NMR titrations, because NMR is adept at detecting weakly interacting ligands; thus, there is a need for additional fluorescence titrations to verify the presence of saturable ligand–protein binding, and to obtain more accurate K_d values when $K_d \ll [\text{protein}]$.

NMR titrations can also provide structural information, based on location of the perturbed amino acid in the 3D structure of the protein, which corresponds to the crosspeak that is perturbed (if chemical shift assignments are available for the protein). Monitoring of chemical shift perturbations of crosspeaks in 2D ^1H – ^{15}N HSQC spectra of PMK indicates there has been substantial movement of residues in the CORE and LID regions shown in Fig. 2 [15]. CSDDD_1633 and CSDDD_2260 both perturb the chemical shift of D163, an important hinge residue between the LID and CORE regions [15]. Also, ligand–PMK binding produced chemical shift perturbations outside of the binding site, suggesting a conformational changes, such as those that could result from motion

around the hinge residue between domains, as we have reported previously [15]. Similar chemical shift perturbations are seen in this study to those that we have reported previously for ATP binding, both at the hinge and outside the ATP binding site, further suggesting that the in-house synthetic compounds are binding similarly to ATP.

Consistent with their binding in a highly basic pocket (intended to accommodate phosphates), all three of the compounds identified have at least two formal negative charges, either on sulfonate groups (CSDDD_1633 and CSDDD_2419) or carboxylic acids (CSDDD_2260). Recently, we observed that molecules with sulfonates could function as bio-mimics for naturally occurring negatively charged ligands with phosphates, sulfates, or post-translationally modified residues (either phosphorylated or sulfated) [37]. Compounds CSDDD_1633 and CSDDD_2419 also contain phenolic groups that would be expected to have low pK_a 's, based on potential for resonance delocalization of negative charge (though an azo group or into a quinine carbonyl). This would put an additional negative charge on these molecules. Thus, all inhibitors are highly charged, making them suitable mimics of the PMK substrates which are also rich with negative charges.

Docking and subsequent titration studies also identified a natural product inhibitor, luteolin, a flavanoid, from the Chemibase collection. Luteolin has modest affinity for PMK, with a K_d of 61 μ M. While it appears that luteolin exhibits no charge, this is probably not accurate. As for two of the compounds reported above, luteolin contains phenolic groups that are likely to be readily ionized, due to resonance delocalization into the carbonyl. Indeed, the phenolic-quinone substructure in CSDDD_1633 is similar to the corresponding substructure in luteolin. Chemical shift perturbation mapping for this compound (Fig. 3) is strikingly different from the in-house compounds. It is therefore possible that luteolin is binding differently than the in-house synthetic chemicals. But, luteolin does cause a large chemical shift perturbation to the active site D163, as expected [15]. Interestingly, luteolin has been reported to show a wide range of biological effects including cardiovascular protection [38], but it is not clear what protein targets are responsible for this effect. It is possible that binding to PMK may at least contribute to the favorable cardiovascular effects of luteolin.

5. Conclusion

In summary, we have identified novel inhibitors of PMK, which possess significant negative charge that is suitable for binding to the highly basic PMK active site. Using virtual screening to identify potential inhibitors, and NMR and fluorescence experiments to verify binding, we found that docking yielded a hit rate of 15% and identifies reasonably potent PMK inhibitors with K_d values in the 6–60 μ M range. These molecules could be useful to investigators as chemical genetic probes or as starting points in further drug and inhibitor design studies.

Acknowledgments

This work was supported by a grant from the Thailand Research Fund (RTA5380010), and P.B. is grateful to The Royal Golden Jubilee PhD Program (PHD/0262/2549) for a scholarship. The National Center of Excellence in Petroleum, Petrochemical Technology and Advanced Materials and KURDI, and Kasetsart University are gratefully acknowledged for providing research facilities. D.S.S. acknowledges support from the American Heart Association (05303072) and an NIH Instrumentation Grant (S10 RR019012). H.M. acknowledges support from NIH (DK53766). Finally, Dr. Chak Sangma is gratefully acknowledged for providing access to Chemibase.

Appendix A. Supplementary data

Supplementary data associated with this article can be found, in the online version, at <http://dx.doi.org/10.1016/j.bbrc.2012.10.130>.

References

- [1] K.L. Chambliss, C.A. Slaughter, R. Schreiner, G.F. Hoffmann, K.M. Gibson, Molecular cloning of human phosphomevalonate kinase and identification of a consensus peroxisomal targeting sequence, *J. Biol. Chem.* 271 (1996) 17330–17334.
- [2] J.L.I. Andreassi, M.W. Vetting, P.W. Bilder, S.L. Roderick, T.S. Leyh, Structure of the ternary complex of phosphomevalonate kinase: the enzyme and its family, *Biochemistry* 48 (2009) 6461–6468.
- [3] E.G. Bliznakov, Diabetes and the role of isoprenoid biosynthesis, *FEBS Lett.* 525 (2002) 169–170.
- [4] C.E. Elson, Suppression of mevalonate pathway activities by dietary isoprenoids: protective roles in cancer and cardiovascular disease, *J. Nutr.* 125 (1995) 1666S–1672S.
- [5] E.S. Istvan, Structural mechanism for statin inhibition of 3-hydroxy-3-methylglutaryl coenzyme A reductase, *Am. Heart J.* 144 (2002) S27–S32.
- [6] G.A. Rodan, R. Balena, Bisphosphonates in the treatment of metabolic bone diseases, *Ann. Med.* 25 (1993) 373–378.
- [7] I. Buhaescu, H. Izzedine, Mevalonate pathway: a review of clinical and therapeutic implications, *Clin. Biochem.* 40 (2007) 575–584.
- [8] T.J. Herdendorf, H.M. Miziorko, Phosphomevalonate kinase: functional investigation of the recombinant human enzyme, *Biochemistry* 45 (2006) 3235–3242.
- [9] S. Bazaes, E. Beytia, A.M. Jabalquinto, F. Solis de Ovando, I. Gomez, J. Eyzaguirre, Pig liver phosphomevalonate kinase. 1. Purification and properties, *Biochemistry* 19 (1980) 2300–2304.
- [10] K. Bloch, S. Chaykin, A.H. Phillips, A. De Waard, Mevalonic acid pyrophosphate and isopentenylpyrophosphate, *J. Biol. Chem.* 234 (1959) 2595–2604.
- [11] S. Ferrand, J. Tao, X. Shen, D. McGuire, A. Schmid, J.F. Glickman, U. Schopfer, Screening for mevalonate biosynthetic pathway inhibitors using sensitized bacterial strains, *J. Biomol. Screening* 16 (2011) 637–646.
- [12] H.M. Miziorko, Enzymes of the mevalonate pathway of isoprenoid biosynthesis, *Arch. Biochem. Biophys.* 505 (2011) 131–143.
- [13] C.W. Muller, G.J. Schlauderer, J. Reinstein, G.E. Schulz, Adenylate kinase motions during catalysis: an energetic counterweight balancing substrate binding, *Structure* 4 (1996) 147–156.
- [14] M. Gerstein, A.M. Lesk, C. Chothia, Structural mechanisms for domain movements in proteins, *Biochemistry* 33 (1994) 6739–6749.
- [15] A.L. Olson, H. Yao, T.J. Herdendorf, H.M. Miziorko, S. Hannongbua, P. Saparpakorn, S. Cai, D.S. Sem, Substrate induced structural and dynamics changes in human phosphomevalonate kinase and implications for mechanism, *Proteins: Struct. Funct. Bioinf.* 75 (2009) 127–138.
- [16] T.J. Herdendorf, H.M. Miziorko, Functional evaluation of conserved basic residues in human phosphomevalonate kinase, *Biochemistry* 46 (2007) 11780–11788.
- [17] D.D. Leipe, E.V. Koonin, L. Aravind, Evolution and classification of P-loop kinases and related proteins, *J. Mol. Biol.* 333 (2003) 781–815.
- [18] E.V. Koonin, A superfamily of ATPases with diverse functions containing either classical or deviant ATP-binding motif, *J. Mol. Biol.* 229 (1993) 1165–1174.
- [19] J.J. Irwin, B.K. Shoichet, ZINC – A free database of commercially available compounds for virtual screening, *J. Chem. Inf. Model.* 45 (2005) 177–182.
- [20] C.N. Cavasotto, A.J.W. Orry, Ligand docking and structure-based virtual screening in drug discovery, *Curr. Top. Med. Chem.* 7 (2007) 1006–1014.
- [21] B.K. Shoichet, Virtual screening of chemical libraries, *Nat. Rev. Mol. Cell Biol.* 432 (2004) 862–865.
- [22] Q. Chang, X. Yan, S. Gu, J. Liu, D. Liang, Crystal structure of human phosphomevalonate kinase at 1.8 Å resolution, *Proteins: Struct. Funct. Bioinform.* 73 (2008) 254–258.
- [23] D.S. Sem, M. Pellecchia, NMR in the acceleration of drug discovery, *Curr. Opin. Drug Discov. Devel.* 4 (2001) 479–492.
- [24] A.L. Olson, S. Cai, T.J. Herdendorf, H.M. Miziorko, D.S. Sem, NMR dynamics investigation of ligand-induced changes of main and side-chain arginine N-H's in human phosphomevalonate kinase, *J. Am. Chem. Soc.* 132 (2010) 2102–2103.
- [25] C. Sangma, D. Chuakheaw, N. Jongkon, S. Gadavani, Computer techniques for drug development from Thai traditional medicine, *Curr. Pharm. Des.* 16 (2010) 1753–1784.
- [26] Thai medicinal plants. <http://Chemibase.ku.ac.th>.
- [27] Accelrys Software, Pipeline pilot, ver. 7.4.
- [28] Molecular Networks, CORINA, ver. 2.4.
- [29] G.M. Morris, D.S. Goodsell, R.S. Halliday, R. Huey, W.E. Hart, R.K. Belew, A.J. Olson, Automated docking using a Lamarckian genetic algorithm and an empirical binding free energy function, *J. Comput. Chem.* 19 (1998) 1639–1662.
- [30] G.M. Morris, R. Huey, W. Lindstrom, M.F. Sanner, R.K. Belew, D.S. Goodsell, A.J. Olson, AutoDock4 and AutoDockTools4: automated docking with selective receptor flexibility, *J. Comput. Chem.* 30 (2009) 2785–2791.

- [31] R. Huey, G.M. Morris, A.J. Olson, D.S. Goodsell, A semiempirical free energy force field with charge-based desolvation, *J. Comput. Chem.* 28 (2007) 1145–1152.
- [32] J. Marley, M. Lu, C. Bracken, A method for efficient isotopic labeling of recombinant proteins, *J. Biomol. NMR* 20 (2001) 71–75.
- [33] E. Gasteiger, C. Hoogland, A. Gattiker, S. Duvaud, M.R. Wilkins, R.D. Appel, A. Bairoch, Protein identification and analysis tools on the ExPASy server, in: *The Proteomics Protocols Handbook*, 2005, pp. 571–607.
- [34] F. Delaglio, S. Grzesiek, G.W. Vuister, G. Zhu, J. Pfeifer, A. Bax, NMRPipe: a multidimensional spectral processing system based on UNIX pipes, *J. Biomol. NMR* 6 (1995) 277–293.
- [35] B.A. Johnson, R.A. Blevins, NMRView: a computer program for the visualization and analysis of NMR data, *J. Biomol. NMR* 4 (1994) 603–614.
- [36] GraphPad Software, ver. 4.0 .
- [37] A.L. Olson, T.S. Neumann, P. Boonsri, J.J. Ziarek, F.C. Peterson, S. Cai, B. Volkman, S. Hannongbua, D.S. Sem, Aryl-sulfonates as biomimetics for negatively charged ligands: Application to phosphomevalonate kinase and the CXCL12 chemokine, *Med. Chem. Comm.* (in preparation).
- [38] M. Lopez-Lazaro, Distribution and biological activities of the flavonoid luteolin, *Mini Rev. Med. Chem.* 9 (2009) 31–59.